Diagnostics of Lateral Mixing in the Ocean

Ryan Abernathey, * David Ferreira and John Marshall(?)

Massachusetts Institute of Technology, Cambridge, Massachusetts, USA

Andreas Klocker

Australian National University, Canberra, Australia

*Corresponding author address: Ryan Abernathey, Department of Earth, Atmospheric, and Planetary Sciences, Massachusetts Institute of Technology, 54-1615 77 Massachusetts Ave., Boston, MA 02139.

E-mail: rpa@mit.edu

ABSTRACT

Enter abstract here.

1. Introduction

The meridional overturning circulation of the ocean plays a fundamental role in the climate system by providing a link between the deep ocean, where vast quantities of heat and carbon can be stored, and the atmosphere (**??**). Much of the global deep water upwells in the Southern Ocean due to Ekman pumping by the surface westerlies, but the wind-driven upwelling is partially cancelled by an eddy-induced circulation (Toggweiler and Samuels 1998; Marshall and Radko 2003; Abernathey et al. 2011; Marshall and Speer 2012).

Despite its importance, direct observation of the MOC is extremely challenging, demanding continuous, high-resolution measurements of the ocean flow field across entire basins and through the full water column. One such attempt has been made in the North Atlantic through the RAPID program, a dense array of moorings and repeat sections along 26.5° N (**??**). However, doubt remains whether even this sophisticated network can distinguish MOC trends from slow internal variability and noise from the eddy field (**?**). Given the remoteness and hostility of the Southern Ocean, it seems unlikely that such direct approaches will ever be implemented there. Instead, various indirect methods will continue to be employed.

A common approach in the Southern Ocean has been to infer distinct components of the MOC in different ways. For instance, Sallée et al. (2010) recently used ARGO data to estimate the steady geostrophic flow, satellite data to calculate the Ekman pumping, and the eddy parameterization of Gent and McWilliams (1990, henceforth referred to as GM) to estimate the eddy-induced advection. The divergence of these three components of the transport across the base of the mixed layer gave the net subduction and upwelling, i.e. the residual MOC.

The isoypcnal mixing rates from DIMES will be very valuable if they can lead to improved estimates of the eddy-induced component MOC in the Southern Ocean. However, the link between observable diagnostics of mixing and the actual eddy-induced transport is somewhat obscure. The studies of Speer et al. (2000) and Sallée et al. (2010) rely on the GM framework to infer the eddy-induced advection, which is based on the lateral diffusivity of

buoyancy. Smith and Marshall (2009) have shown that this quantity can differ significantly from the diffusivity of potential vorticity or passive tracers. Smith and Marshall (2009) and Abernathey et al. (2010) also demonstrated that mixing rates in the Southern Ocean vary strongly with depth, a fact that further upsets the equivalence between GM and potential vorticity mixing.

The goal of this paper is to compare various methods of diagnosing lateral mixing and assess which diagnostics are the most useful. Some of these diagnostics are possible only in the context of a numerical model, in which all the dynamical fields are known exactly. We call these *perfect* diagnostics. But there are less precise diagnostics have been or could potentially be applied to the real ocean, for example, in the recent DIMES experiment. We call these *practical* diagnostics.

[[[Need to improve and expand the intro.]]]

2. Numerical Model

[[[Needs to be written.]]]

3. Perfect Mixing Diagnostics

The *perfect* mixing diagnostics are quantities which can be calculated only with very detailed synoptic observation of the flow. Such diagnostics provide the most complete characterization of mixing and transport possible. They are straightforward to extract from numerical models but nearly impossible for the real ocean. (In the atmosphere, where extensive reanalysis products provide sufficient spatial and temporal resolution, many perfect diagnostics can be calculated.)

Observational problems aside, the interpretation of perfect mixing diagnostics still poses a challenge. Different diagnostics have been used throughout the literature to characterize eddy

mixing, and the relationship between these diagnostics is not always obvious. Our purpose here is to consolidate many different diagnostics in one place and show their relationship. A similar study was made for the atmosphere by Plumb and Mahlman (1987, henceforth PM87), who also review some theoretical aspects. Here we basically repeat their methodology for an ACC-like flow. In the next section, we will compare the perfect diagnostics with *practical* diagnostics, that is, diagnostics which there is some hope of obtaining from the real ocean.

a. Passive Tracers

Our starting point is to examine the mixing of passive tracers. Passive tracers obey an advection-diffusion equation of the form

$$\frac{\partial c}{\partial t} + \boldsymbol{v} \cdot \nabla c = \kappa \nabla^2 c + C \tag{1}$$

where c is the tracer concentration, $\boldsymbol{u}$ is the velocity field, κ is a small-scale diffusivity, and C is a source or sink. We will focus on cases where $C = 0$ and the diffusive term is negligible for the large-scale budget of c. (Some small-scale diffusion is necessary for mixing to occur, and likewise it is impossible to eliminate diffusion completely from numerical models. But for flows of large Peclét number, diffusion is an important term only in the tracer *variance* budget, not the tracer budget itself.)

1) Diffusivity Tensor

PM87 performed a detailed study of the transport characteristics of a model atmosphere using passive tracers. Here we briefly review their definition of $\mathbf{K}$, the diffusivity tensor, which we view as the most complete diagnostic of eddy-transport. The reader is referred to PM87 for a more in-depth discussion.

Taking a zonal average of (1) (indicated by an overbar) and neglecting the RHS terms,

we obtain

$$\frac{\partial \overline{c}}{\partial t} + \overline{\boldsymbol{v}} \cdot \nabla \overline{c} = -\nabla \cdot \boldsymbol{F}_c \tag{2}$$

where $\boldsymbol{F}_c = (\overline{v'c'}, \overline{w'c'})$ is the eddy flux of tracer in the meridional plane. The tensor diffusivity $\mathbf{K}$ relates this flux to the background gradient in each direction; it is defined by

$$\boldsymbol{F}_c = -\mathbf{K} \cdot \nabla \overline{q} \ . \tag{3}$$

This equation is underdetermined for a single tracer, but PM87 thought to use multiple tracers with different background gradients to calculate it. This method has also recently been applied by **?**.

We found $\mathbf{K}$ by solving (3) for six independent tracers. In this case, (3) is overdetermined, and the "solution" is a least-squares best fit. The initial tracer concentrations used were as follows: $c_1 = y$, $c_2 = z$, $c_3 = \cos(\pi y/L_y)\cos(\pi z/H)$, $c_5 = \sin(\pi y/L_y)\sin(\pi z/H)$, $c_5 = \sin(\pi y/L_y)\sin(2\pi z/H)$, $c_6 = \cos(2\pi y/L_y)\cos(\pi z/H)$. (We experimented with different initial concentrations, but found the results to be insensitive to this detail, provided many tracers with different gradients were used.) The tracers were allowed to evolve from these initial conditions for one year. (An experiment with two years of evolution produced very similar results.) $\boldsymbol{F}_c$ and $\nabla \overline{c}$ were calculated for each tracer by performing a zonal and time average over the one-year period and then over an ensemble of 20 different years. In matrix form, the equation solved to find $\mathbf{K}(y,z)$ was

$$\begin{bmatrix} \overline{v'c'_1} & \overline{v'c'_2} & ... & \overline{v'c'_6} \\ \overline{w'c'_1} & \overline{w'c'_2} & ... & \overline{w'c'_6} \end{bmatrix} = - \begin{bmatrix} K_{yy} & K_{yz} \\ K_{zy} & K_{zz} \end{bmatrix} \begin{bmatrix} \partial\overline{c_1}/\partial y & \partial\overline{c_2}/\partial y & ... & \partial\overline{c_6}/\partial y \\ \partial\overline{c_1}/\partial z & \partial\overline{c_2}/\partial z & ... & \partial\overline{c_6}/\partial z \end{bmatrix} \tag{4}$$

where each element of $\mathbf{K}$ at each point in (y,z) space is a least-squares estimate that minimizes the error across all tracers.

It is most informative to decompose $\mathbf{K}$ into two parts,

$$\mathbf{K} = \mathbf{L} + \mathbf{D} \ , \tag{5}$$

where $\mathbf{L}$ is an antisymmetric tensor and $\mathbf{D}$ is symmetric. Because the flux due to $\mathbf{L}$ is normal to $\nabla \overline{q}$, its effects are advective, rather than diffusive (Plumb 1979, PM87). Using this fact,

we can rewrite (2) as

$$\frac{\partial \overline{c}}{\partial t} + (\overline{\boldsymbol{v}} + \boldsymbol{v}^*) \cdot \nabla \overline{c} = \nabla \cdot (\mathbf{D} \cdot \nabla \overline{q}) \tag{6}$$

where $\boldsymbol{v}^* = (v^*, w^*)$ is an eddy-induced effective transport velocity, defined by a streamfunction χ, such that

$$v^* = -\partial\chi/\partial z \ , \quad w^* = \partial\chi/\partial y \tag{7}$$

and

$$\mathbf{L} = \begin{bmatrix} 0 & -\chi \\ \chi & 0 \end{bmatrix} \ . \tag{8}$$

Under adiabatic conditions, χ is approximatey equal to the transformed-eulerian-mean eddy-induced streamfunction, or the "bolus transport" stream function in thickness-weighted isopycnal coordinates. Again, for more detailed discussion, the reader is referred to PM87.

Because $\mathbf{L}$ is advective in nature (and doesn't appear in the tracer variance budget), all of the actual *mixing* due to eddies in contained in $\mathbf{D}$. Since $\mathbf{D}$ is symmetric, it can be diagonalized by rotation through an angle α where

$$\tan 2\alpha = \frac{2D_{yz}}{D_{yy} - D_{zz}}. \tag{9}$$

The rotated matrix,

$$\mathbf{D}' = \begin{bmatrix} D'_{yy} & 0 \\ 0 & D'_{zz} \end{bmatrix} = \begin{bmatrix} \cos\alpha & -\sin\alpha \\ \sin\alpha & \cos\alpha \end{bmatrix} \mathbf{D} \tag{10}$$

describes the eddy diffusion along (D'_{yy}, the *major-axis* diffusivity) and across (D'_{zz}, the *minor-axis* diffusivity) the plane defined by α, which we call the *mixing angle*.

We have seen that the physical interpretation of $\mathbf{K}$ is best summarized by four quantities: χ, α, D'_{yy}, and D'_{zz}. These quantities are plotted in Fig. 1. We see that the mixing angle is along isopycnals throughout most of the domain, except close the surface, where the mixing acquires a more horizontal character. This pattern is consistent with the paradigm that ocean eddies mix adiabatically in the interior and diabolically in the "surface diabetic

layer," i.e. the layer over which isopycnals outcrop (Treguier et al. 1997). Consequently, D'_{yy} can be described as an *isopycnal* mixing coefficient, and D'_{zz} as *diapycnal* mixing.

An obvious feature in the spatial structure of D'_{yy} is pronounced peak at mid-depth (approx. 1200 m). Enhanced lateral mixing at a mid-depth *critical layer* is a general feature of baroclinically unstable jets (Green 1970; Killworth 1997). Many studies have confirmed the presence of an enhanced mid-depth mixing layer in the ACC (Smith and Marshall 2009; Abernathey et al. 2010; Klocker et al. 2011). Our highly idealized model evidently shares this behavior. It is also important to note, though, that D'_{yy} varies even more strongly with y, with the strongest mixing being in the "storm track" at the center of the channel.

The interpretation of D'_{zz} is more puzzling. The major-axis diffusivity is much greater than the minor: $|D'_{yy}|/|D'_{zz}| \simeq 10^7$. Combined with the fact that α departs only very slightly from 0 (due to the aspect ratio of the domain), this means that $D'_{yy} \simeq D_{yy}$. On the other hand, each individual component of $\mathbf{D}$ is much greater in magnitude than D'_{yy}, whose value depends on large cancellations in (10). The implied diapycnal diffusivity of $O(10^-4)$ m^2 s^{-1} is at odds with a previous study focused exclusively on diapycnal mixing (**?**), which found values of $O(10^-5)$ m^2 s^{-1} and below in the exact same model. Our conclusion is that small errors in α cause D'_{zz} to be polluted with spurious large values, and that the multiple-tracer method described here is not a good diagnostic of diapycnal mixing. *[[[How can we improve this argument?]]]* Regardless, the focus of the present study is on lateral mixing, and we will not concern ourselves with D'_{zz} further here.

Say something about χ. Griffies (1998).

2) Nakamura Effective Diffusivity

The framework developed by Nakamura (1996) has gained widespread use in assessing lateral mixing in the ocean and atmosphere (Nakamura and Ma 1997; Haynes and Shuckburgh 2000a,b; Marshall et al. 2006; Abernathey et al. 2010; **?**). This framework is relies on a tracer-based coordinate system, in which the flux across tracer isosurfaces can be charac-

terized by an effective diffusivity, which depends only on the instantaneous tracer geometry. The same concept was developed by Winters and D'Asaro (1996) and subsequently applied by **?** to diagnose the temporal evolution of diapycnal mixing in an internal-wave-breaking scenario.

The effective diffusivity is defined as

$$K_{eff} = \kappa \frac{L_e^2}{L_{min}^2} \tag{11}$$

where...blah blah blah. Do we really have to repeat this shit again?

As described in the preceding section, the model was constructed to be as adiabatic as possible, with explicit horizontal and vertical diffusion set to zero. However, the effective diffusivity framework requires a constant small-scale background horizontal diffusivity. Therefore, in the tracer advection for the effective diffusivity experiments, we used an explicit horizontal diffusivity of 50 $\mathrm{m}^2\ \mathrm{s}^{-1}$. Analysis of the tracer variance budget indicated that numerical diffusion elevated this value slightly, to 55 $\mathrm{m}^2\ \mathrm{s}^{-1}$. We performed our experiments by initializing a passive tracer with concentration $c = y$ and allowing it to evolve under advection and diffusion for two years. Every month, a snapshot of c and T was output. This procedure was repeated for 10 consecutive two-year periods, to create a smooth ensemble-average picture of the evolution of K_{eff} over two years.

The 3D tracer field must be sliced into 2D surfaces in order to compute $K_{eff}(y)$. The most straightforward way to accomplish this is to examine surfaces of c at constant z; we call this K_{eff}^H. However, since the mixing angle is along isopycnals, a more physically relevant choice is to project c into isopycnal coordinates; the effective diffusivity computed from this projection we call K_{eff}^{iso}. Abernathey et al. (2010) tried both methods, and here we do the same. Not surprisingly, we see a better match between K_{eff}^{iso} and D'_{yy}.

After two months, the overall magnitude of both K_{eff} calculations stabilizes and remains roughly constant, as does the spatial structure of K_{eff}^{iso}. The spatial structure of K_{eff}^H, on the other hand, continues to evolve over the two year period, departing further and further from K_{eff}^{iso}. The results of one K_{eff} ensemble calculation (at 10 months) are shown in Fig.

2. Comparing this figure with Fig. 1, we see that K^{iso}_{eff} is quite similar in magnitude and spatial structure to D'_{yy}. This agreement between these two diagnostics, based on quite different methods, is expected but nevertheless encouraging. K^{H}_{eff}, on the other hand, while having the right general magnitude, has significant differences in spatial structure. From this we conclude that K^{H}_{eff} is somewhat misleading diagnostic whose physical interpretation is unclear. K^{iso}_{eff}, on the other hand, seems like a robust diagnostic of isopycnal mixing.

b. Active Tracers

Here we compute flux-gradient diffusivities for active tracers. Active tracers are tracers which obey (1) but which also affect the dynamics of the flow. The active tracers we consider are buoyancy and potential vorticity. Unlike the passive tracers, these active tracers are forced at the surface, and their zonal means have reached a steady-state equilibrium. Therefore, it is interesting to ask whether they experience the same diffusivity as the passive tracers.

1) Buoyancy Diffusivity

A simple and widely-used diagnostic of eddy mixing is the horizontal buoyancy diffusivity, defined as

$$K_b = -\frac{\overline{v'b'}}{\overline{b}_y} \ . \tag{12}$$

This quantity plays a central role in the Gent and McWilliams (1990) eddy parameterization. Fig. 3 *[[[More needed.]]]*

2) QGPV Diffusivity

Shown in Fig. **??**. *[[[More needed.]]]*

3) Isopycnal Ertel PV Diffusivity

Have not done this calculation! Is it necessary?

4. Practical Mixing Diagnostics

a. Lagrangian Diffusivity

b. Tracer Release

c. Comparison of All Diagnostics

5. 2D Model

6. Conclusions

Acknowledgments.

Start acknowledgments here.

APPENDIX

Appendix Title Is Entered Here (Primary heading)

a. First appendix secondary heading

b. Second appendix secondary heading

1) First appendix tertiary heading

2) Second appendix tertiary heading

(i) First appendix quaternary heading

(ii) Second appendix quaternary heading

REFERENCES

Abernathey, R., J. Marshall, and D. Ferreira, 2011: The dependence of southern ocean meridional overturning on wind stress. *J. Phys. Oceanogr.*, **41 (12)**, 2261–2278.

Abernathey, R., J. Marshall, E. Shuckburgh, and M. Mazloff, 2010: Enhancement of mesoscale eddy stirring at steering levels in the southern ocean. *J. Phys. Oceanogr.*, 170–185.

Gent, P. and J. McWilliams, 1990: Isopycnal mixing in ocean circulation models. *J. Phys. Oceanogr.*, **20**, 150–155.

Green, J. S., 1970: Transfer properties of the large-scale eddies and the general circulation of the atmosphere. *Quart. J. Roy. Meteor. Soc.*, **96**, 157–185.

Griffies, S. M., 1998: The gent-mcwilliams skew flux. *J. Phys. Oceanogr.*, **28**, 831–841.

Haynes, P. and E. Shuckburgh, 2000a: Effective diffusivity as a diagnostic of atmospheric transport. part i: stratosphere. *J. Geophys. Res*, **105**, 22 777–22 794.

Haynes, P. and E. Shuckburgh, 2000b: Effective diffusivity as a diagnostic of atmospheric transport. part ii: Troposphere and lower stratosphere. *J. Geophys. Res*, **105**, 795–810.

Killworth, P. D., 1997: On the parameterization of eddy transfer: Part i: Theory. *J. Marine Res.*, **55**, 1171–1197.

Klocker, A., R. Ferrari, and J. H. LaCasce, 2011: Estimating supression of eddy mixing by mean flows. *J. Phys. Oceanogr.*

Marshall, J. and T. Radko, 2003: Residual mean solutions for the antarctic circumpolar current and its associated overturning circulation. *J. Phys. Oceanogr.*, **33**, 2341–2354.

Marshall, J., E. Shuckburgh, H. Jones, and C. Hill, 2006: Estimates and implications of surface eddy diffusivity in the southern ocean derived from tracer transport. *J. Phys. Oceanogr.*, **36**, 1806–1821.

Marshall, J. and K. Speer, 2012: Closing the meridional overturning circulation through southern ocean upwelling. *Nature Geoscience*, **5**, 171–180.

Nakamura, N., 1996: Two-dimensional mixing, edge formation, and permeability diagnosed in an area coordinate. *J. Atmos. Sci.*, **53**, 1524–1537.

Nakamura, N. and J. Ma, 1997: Modified lagrangian-mean diagnostics of the stratospheric polar vortices 2. nitrous oxide and seasonal barrier migration in the cryogenic limb array etaion spectrometer and skyhi general circulation model. *J. Geophys. Res.*, **102**, 25,721–25,735.

Plumb, R. A., 1979: Eddy fluxes of conserved quantities by small-amplitude waves. *J. Atmos. Sci.*, **36**, 1699–1705.

Plumb, R. A. and J. D. Mahlman, 1987: The zonally-averaged transport characteristics of the gfdl general circulation/tracer model. *J. Atmos. Sci.*, **44**, 298–327.

Sallée, J. B., K. Speer, S. Rintoul, and S. Wijffels, 2010: Southern ocean thermocline ventilation. *J. Phys. Oceanogr.*, **40**, 509–530.

Smith, K. S. and J. Marshall, 2009: Evidence for enhanced eddy mixing at mid-depth in the southern ocean. *J. Phys. Oceanogr.*, **39**, 50–69.

Speer, K., S. Rintoul, and B. Sloyan, 2000: The diabatic deacon cell. *J. Phys. Oceanogr.*, **30**, 3212–3223.

Toggweiler, J. R. and B. Samuels, 1998: On the ocean's large-scale circulation near the limit of no vertical mixing. *J. Phys. Oceanogr.*, **28**, 1832–1853.

253 Treguier, A. M., I. Held, and V. Larichev, 1997: Parameterization of quasigeostrophic eddies
254 in primitive equation ocean models. *J. Phys. Oceanogr.*, **27**, 567–580.

255 Winters, K. and E. D'Asaro, 1996: Diascalar flux and the rate of fluid mixing. *J. Fluid*
256 *Mech.*, **317**, 179–193.

List of Tables

TABLE 1. This is a sample table caption and table layout. Enter as many tables as necessary at the end of your manuscript. Table from Lorenz (1963).

N	X	Y	Z
0000	0000	0010	0000
0005	0004	0012	0000
0010	0009	0020	0000
0015	0016	0036	0002
0020	0030	0066	0007
0025	0054	0115	0024

List of Figures

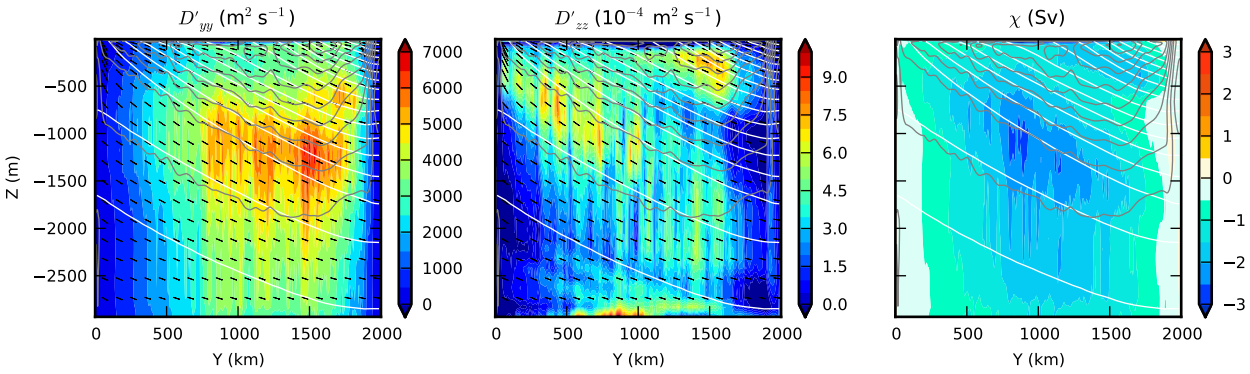

FIG. 1. Decomposition of eddy diffusivity tensor $\mathbf{K}$ into a major-axis diffusivity D'_{yy}, minor-axis diffusivity D'_{zz}, and eddy-induced transport stream function χ. χ has been converted to Sv by multiplying by L_x. The mean isopycnals are shown in white contours (contour interval 0.5° C), and the thermal-wind component of the zonal-mean velocity is shown in grey (contour interval 1 cm s^{-1}). In the left two panels, the mixing angle α is indicated by the black dashes. See text for discussion.

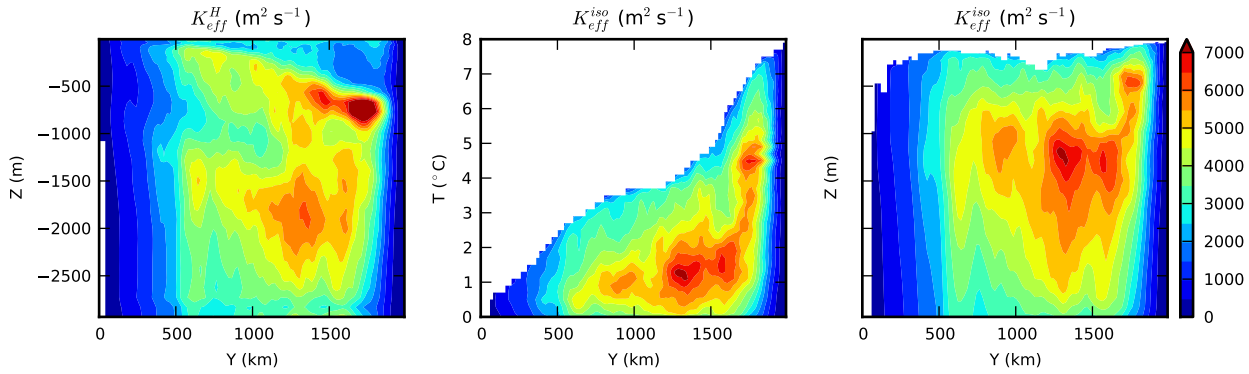

FIG. 2. Nakamura effective diffusivity calculated on a passive tracer after 10 months of evolution. Values shown are an average over an ensemble of 10 independent tracer-release experiments. In the left panel, K^H_{eff} was calculated on slices of c at constant z (horizontal). In the middle panel, K^{iso}_{eff} was calculated on slices of c at constant T (isopycnal). The right panel shows K^{iso}_{eff} mapped back to depth space using the mean isopycnal depths.

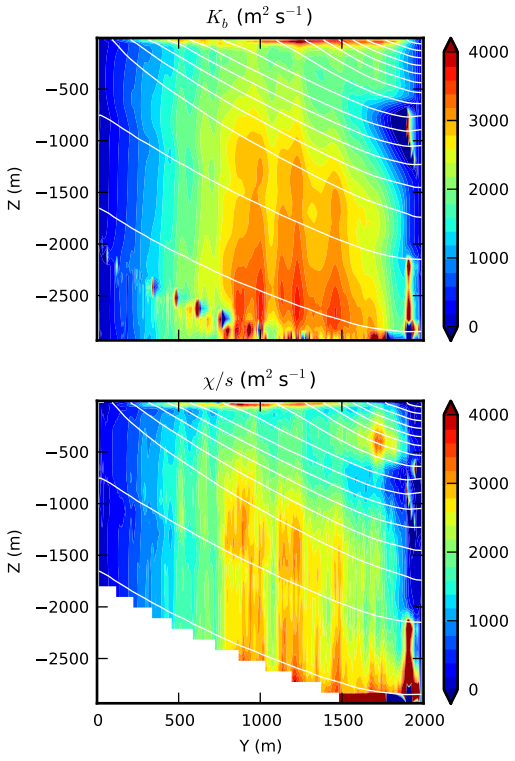

FIG. 3. Left panel: horizontal buoyancy diffusivity K_b calculated from (**??**). Right panel: The equivalent quantity implied by χ.

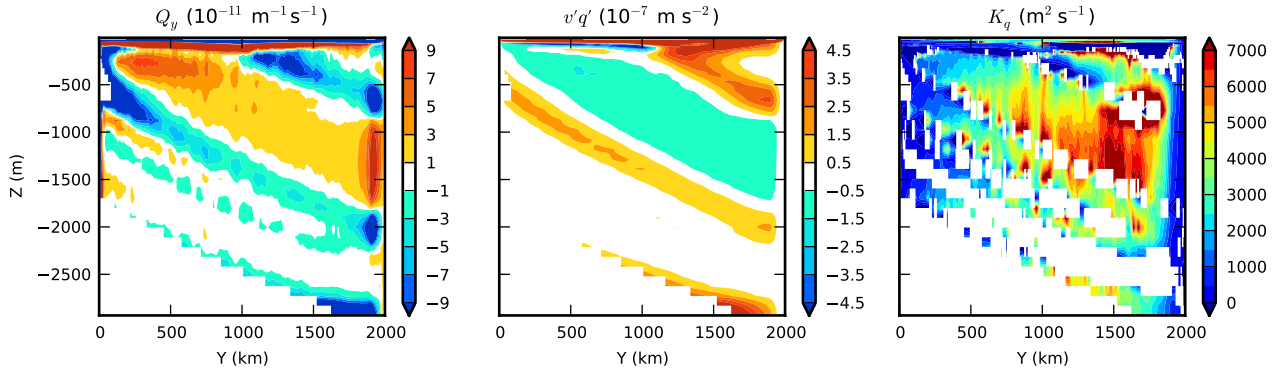

FIG. 4. Left panel: mean qgpv gradient Q_y. Middle: eddy qgpv flux $\overline{v'q'}$. Right: qgpv diffusivity K_q.